scientific reports

OPEN

Innate spectral preferences and aversive visual learning reveal wavelength-dependent preferences and discrimination in *Drosophila melanogaster*

Yoichi Seki✉, Yasuhiro Toriitsuka, Tamaki Yamada, Ayaka Tanaka, Masahiro Mitsumasu, Takako Morimoto & Junji Yamauchi

Chromatic information is detected by distinctly tuned photoreceptors and used in both innate and learned behaviors. Although the molecular identities and spectral sensitivities of these photoreceptors have been extensively characterized, how they combine to function remains elusive. We conducted innate spectral preference and visual learning assays in *Drosophila melanogaster*, a well-established model for exploring the neural mechanisms underlying behaviors. First, we assessed spectral preferences based on slow phototactic responses using combinations of monochromatic LED lights ranging from 402 nm to 630 nm. Flies showed a preference for moderately longer wavelengths (green to orange) over shorter wavelengths (violet to blue). Next, we performed an aversive heat conditioning assay to test wavelength discrimination using the same set of light combinations. Flies successfully learned to discriminate between light stimuli within the short to middle wavelengths (violet to green), but failed to discriminate stimuli within the middle to long wavelengths (green to red). Furthermore, these discrimination behaviors were compared to distances in photoreceptor space, suggesting that the photoreceptor space defined by the two opponent channels—short (Rh3/Rh4) vs. long (Rh6), and middle (Rh5) vs. short (Rh3/Rh4) and long (Rh6)—can effectively predict the behavioral results.
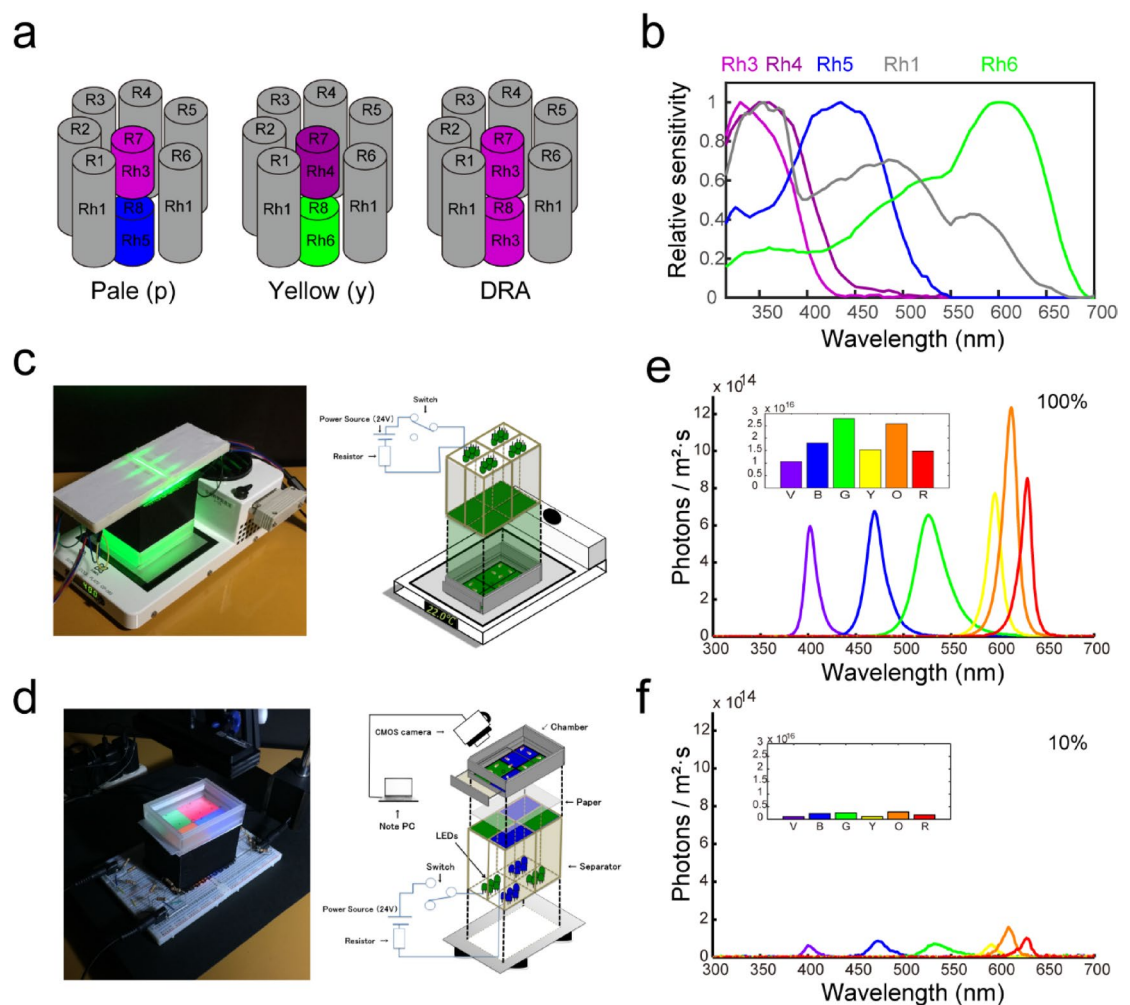
The visual systems of many animals consist of photoreceptors with distinct spectral sensitivities[1]. A particular photoreceptor or photoreceptors is primarily used for detecting achromatic information related to spatial and temporal changes in luminance, such as form and motion perception, while another (or partly overlapping) set of photoreceptors contributes to processing chromatic information, enabling color perception[2]. Narrow band sensitivity is advantageous for wavelength discrimination but causes a low signal-to-noise ratio, leading to the convergence of a small set of photoreceptors with sensitivities of approximately 100 nm half-bandwidth[3,4]. Although molecular identities and spectral sensitivities of photoreceptors have been extensively characterized, how these spectrally distinct photoreceptors combine to function is not fully understood[1,5].

Animal color vision behavior is divided into innate and learned behaviors. The former includes 'wavelength-specific behaviors', primitive forms of which are phototaxis and spectral preference, usually intensity-dependent, whereas the latter includes 'true color vision,' in which discrimination of wavelengths is independent of intensity and often requires spatial vision and an internal representation of color[6,7]. The intensity of input from a specific photoreceptor, or the summation of inputs from a small subset of photoreceptors, could be important for wavelength-specific behaviors, whereas the comparisons between differently tuned photoreceptors by color-opponent neurons could be crucial for true color vision. Although the basic circuitry of the visual system has been elucidated in many animals, the possibility that different sets of photoreceptors are responsible for different behavioral tasks makes the pursuit of the underlying brain circuits very complicated.

The fruit fly *Drosophila melanogaster* is an excellent model for circuit-level analysis of visual behaviors[7–10]. The visual system of *D. melanogaster* comprises a pair of compound eyes, each containing approximately 750 ommatidia, and three small ocelli. In higher flies (Diptera), the compound eyes exhibit a unique organization known as neural superposition[11,12]. Five classes of photoreceptors have been identified: two ultraviolet (UV)-sensitive, blue-sensitive, green-sensitive, and broadband-sensitive photoreceptors (color terms are used according

Laboratory of Molecular Neuroscience and Neurology, School of Life Sciences, Tokyo University of Pharmacy and Life Sciences, 1432-1 Horinouchi, Hachioji, Tokyo 192- 0392, Japan. ✉email: yseki@toyaku.ac.jp

to the human perception throughout the manuscript). In *D. melanogaster*, ommatidia are typically classified into three subtypes: pale and yellow types, which are stochastically distributed in a 35:65 (p: y) ratio, and dorsal rim area (DRA) ommatidia, which are localized in the dorsal-most region of the compound eye and are specialized for detecting polarized light from the sky[13] (Fig. 1a). The spectral sensitivities of the photoreceptors have been well characterized (Fig. 1b)[14,15]. The outer R1–R6 photoreceptor cells express the broadband-sensitive Rh1 photoreceptor and project short visual fibers to the lamina. R7 photoreceptor cells express short UV-sensitive Rh3 in R7p and long UV-sensitive Rh4 in R7y, while R8 photoreceptor cells express blue-sensitive Rh5 in R8p and green-sensitive Rh6 in R8y. Both inner R7 and R8 photoreceptor cells form long visual fibers that project to the medulla. Notably, DRA ommatidia express Rh3 in R8[16], while yellow-type ommatidia in the dorsal third of the compound eye co-express Rh3 and Rh4 in R7y[17]. In flies, as in birds, achromatic and chromatic vision have long been considered distinctly separated, with broadband Rh1 expressed in R1–6 and narrow-band Rh3–6 expressed in R7 and 8[2]. Due to the advantage of narrow spectral tuning for color discrimination, R7 and R8 photoreceptors play key roles in chromatic information processing, as proposed by Troje[18]. However, subsequent studies have suggested interactions between the inner and outer photoreceptors[19,20]. In addition to the conventional photoreceptors found in the compound eyes, several extra-retinal photoreceptors or photosensitive molecules have been identified[21]. Rh7, which is sensitive to blue and violet light, is expressed in R8 photoreceptors of the compound eyes, in certain circadian clock neurons in the brain, and in the Hofbauer-

Fig. 1. Photoreceptors in *D. melanogaster* and experimental setups. **a**. Schematic diagram of the organization of the photoreceptors in the compound eyes of the fly. **b**. Spectral sensitivity of the photoreceptors adapted from[15]. **c**. Experimental setup for conditioning. The fly chamber placed on the cool plate is illuminated by LEDs on the bread board from above. Schematic diagram of the setup is shown on the right. **d**. Experimental setup for testing. The fly chamber is illuminated by LEDs on the bread board from below. Schematic diagram of the setup is shown on the right. During the tests, the flies moved freely within the chamber, which was illuminated by two light stimuli projected diagonally opposite each other (or in parallel during pilot experiments). **e**. Photon counts of each LED stimulus at bright intensity (~ 100%). Inset shows integrals of the photon counts for each stimulus. **f**. Photon counts of each LED stimulus at dim intensity (~ 10%). Inset shows integrals of the photon counts for each stimulus.

Buchner (HB) eyelet—an additional light-sensing organ located between the lamina and medulla—where it is co-expressed with Rh6[22–24]. Cryptochrome, a blue- and UV-light-sensitive photopigment, is expressed in circadian clock neurons and the compound eyes[25–28]. Furthermore, a recent study reported transient receptor potential (TRP) channels, including Painless, TrpA1, and Pyrexia may be involved in spectral preference behaviors[29]. Many of these molecules are known to play important roles in light entrainment of circadian rhythms and may also influence both innate and learned chromatic behaviors.

The spectral preferences of *D. melanogaster* have been extensively studied in combination with photoreceptor mutants and genetic manipulations, revealing the roles of specific photoreceptors in mediating phototactic behaviors[30–36]. Conventionally, fly phototactic behavior has been classified into two types: fast phototaxis and slow phototaxis. Fast phototaxis is an immediate response to light, typically observed when flies are alert and disturbed[30,32,35–38]. This behavior reflects an escape reaction, with flies showing a preference for shorter wavelengths as an indicator of open sky. Conversely, slow phototaxis is a delayed response occurring over longer period, observed when flies are free to move and choose between two differently illuminated areas[29,33,34]. Spectral preference in slow phototactic behavior has not been consistently determined and varies depending on the assay.

In contrast, true color vision in *D. melanogaster* has been demonstrated through learned discrimination behaviors. Associative visual learning assays are essential for evaluating the ability of flies to distinguish between different wavelengths of light, independent of intensity. These assays typically involve conditioning with aversive stimuli, such as electric shocks[39,40] shaking[41,42] or heat[43,44] or with appetitive stimuli, such as sucrose[19] to assess color discrimination. Previous studies have shown that flies can learn to discriminate between different color combinations, such as blue vs. yellow[40,41] or blue vs. green[19,43,44]. Notably, only one study has tested a relatively wide range of color combinations (406–606 nm, 8 different wavelengths) and reported a spectral discrimination function[42]. Additionally, several studies have shown that flies are capable of learning intensity differences[19,45,46]. A recent study demonstrated that not only the combination of Rh3–6, but also the parings such as Rh1 and Rh4, or Rh4 and Rh6 alone, can support discrimination between blue and green[19]. These findings suggest that multiple photoreceptor types contribute to color discrimination in *D. melanogaster*. However, the underlying mechanisms remain poorly understood.

In this study, we developed a two-choice behavioral assay to examine both innate preferences and learned discrimination in flies using various combinations of light wavelengths. The slow phototactic responses and visual learning performances were found to be dependent on the spectral properties of the stimuli. We then compared the learned discrimination behaviors with photoreceptor space representations to assess how different photoreceptor types might be functionally combined. Our findings provide valuable foundational data for further investigating the neural computations underlying spectral processing in this important model animal.

Results

In this study, we evaluated the ability of wild-type Canton-S flies to discriminate six different monochromatic lights. We developed an associative learning paradigm comprising a conditioning apparatus (Fig. 1c), in which light stimulus was paired with aversive heat, and a test apparatus (Fig. 1d), in which flies chose between two distinct areas illuminated by different light stimuli. The six monochromatic lights were generated using LEDs of six different colors at two intensity levels, and their spectral properties are shown in Fig. 1e and f (detailed LED properties are provided in Supplementary Table S1).

Before conducting learning-based discrimination tests for all pairwise combinations of the six LED colors, we first assessed innate spectral preferences using the test apparatus alone, without conditioning. We then carried out a series of pilot experiments to establish and validate the learning paradigm. Finally, we performed behavioral tests to assess learned color discrimination and evaluated the results in terms of photoreceptor contributions.
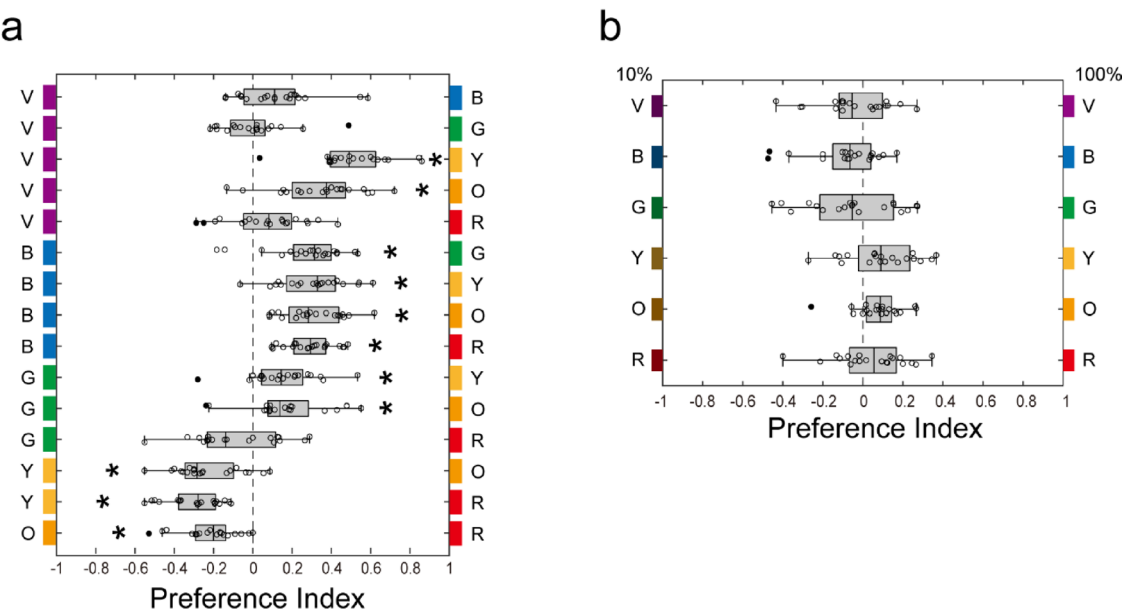
Spectral preference through slow phototactic behavior

First, we examined innate spectral preferences using combinations of six monochromatic lights (λmax = 402 nm (violet), 470 nm (blue), 526 nm (green), 596 nm (yellow), 613 nm (orange), 630 nm (red)) (Fig. 1e). The distribution of flies after two minutes of free walking was quantified as a preference index. We therefore classified these behaviors as slow phototactic responses. Flies exhibited a positive preference for green, yellow, and orange when presented alongside blue or violet, with the exception of violet vs. green (blue vs. green, PI = -0.274 ± 0.043 (mean ± SEM), p = 2.19.E-04; blue vs. yellow PI = -0.307 ± 0.038, p = 1.78.E-07; blue vs. orange, PI = -0.306 ± 0.034, p = 3.15.E-08; violet vs. green, PI = -9.71.E-05 ± 0.037, p = 6.87.E-01; violet vs. yellow, PI = -0.512 ± 0.041, p = 1.59.E-10; violet vs. orange, PI = -0.343 ± 0.048, p = 9.82.E-07; all comparisons were conducted with n = 20 flies; Fig. 2a, statistical details are provided in Table 1). This indicates that flies prefer moderately longer wavelengths (green to orange) and avoid shorter wavelengths (violet to blue).

Next, to evaluate the effects of light intensity, we tested a 1:10 intensity ratio difference across all six wavelengths (Figs. 1e, f). Flies did not show a significant preference for either brighter or darker intensities in any wavelength combination (violet 100% vs. 10%, PI = -0.0392 ± 0.040, p = 3.35.E-01; blue 100% vs. 10%, PI = -0.0873 ± 0.040, p = 5.93.E-02; green 100% vs. 10%, PI = -0.0498 ± 0.050, p = 3.31.E-01; yellow 100% vs. 10%, PI = 0.0918 ± 0.038, p = 2.74.E-02; orange 100% vs. 10%, PI = 0.0749 ± 0.026, p = 1.03.E-02; red 100% vs. 10%, PI = 0.0406 ± 0.040, p = 3.27.E-01; all comparisons were conducted with n = 20 flies; Fig. 2b, statistical details are provided in Table 2). These results indicate that spectral preference in this slow phototactic assay is largely independent of light intensity.

Visual learning assay using heat as an aversive stimulus

To evaluate the discrimination between two different monochromatic light stimuli, we employed a classical conditioning assay. Monochromatic LED light served as the conditioned stimulus (CS), and aversive temperature was used as the unconditioned stimulus (US). Differential conditioning was applied to test the discrimination

Fig. 2. Innate preference for combinations of six monochromatic lights through slow phototactic behaviors. **a**. Spectral preference for each combination of six monochromatic LEDs (violet, blue, green, yellow, orange, and red) ($n = 20$). **b**. Preference for intensity differences in six monochromatic wavelengths ($n = 20$). The intensity difference is approximately 1:10 (see Figs. 1E, F). Statistically significant differences from zero were assessed with a one sample t-test or a Wilcoxon signed-rank test. $*p < 0.05$, after p-values were Bonferroni corrected. Mean values and other statistical information are summarized in Tables 1 and 2.

	combinations	mean PI	SEM	n	p value	$p < \alpha$
1	V vs. B	-0.126	0.044	20	1.02.E-02	n.s
2	V vs. G	-9.71.E-05	0.037	20	6.87.E-01†	n.s
3	V vs. Y	-0.512	0.041	20	1.59.E-10	*
4	V vs. O	-0.343	0.048	20	9.82.E-07	*
5	V vs. R	-0.071	0.044	20	1.22.E-01	n.s
6	B vs. G	-0.274	0.043	20	2.19.E-04†	*
7	B vs. Y	-0.307	0.038	20	1.78.E-07	*
8	B vs. O	-0.306	0.034	20	3.15.E-08	*
9	B vs. R	-0.291	0.027	20	1.86.E-09	*
10	G vs. Y	-0.152	0.039	20	8.58.E-04	*
11	G vs. O	-0.171	0.047	20	1.65.E-03	*
12	G vs. R	0.084	0.049	20	1.05.E-01	n.s
13	Y vs. O	0.233	0.038	20	6.35.E-06	*
14	Y vs. R	0.298	0.031	20	8.97.E-09	*
15	O vs. R	0.223	0.032	20	1.12.E-06	*

Table 1. Preference index (PI) for spectral preference between pair of six LED colors. V, violet; B, blue; G, green; Y, yellow; O, orange; R, red; PI, preference index. One sample t-tests were used to assess differences from zero; statistical significance is indicated by asterisks (*) for $p < 0.05$ after Bonferroni correction (adjusted $\alpha = 0.0033$) †Wilcoxon signed-rank tests were used when data violated the assumption of normality (Shapiro-Wilk test).

between the two different light stimuli: one was paired with aversive temperature, and the other with normal temperature.

To determine optimal conditions for the discrimination assay, several variations in the US temperature (34,36, or 39˚C), the duration and repetition of the training (120 s × 4, 60 s × 6, or 30 s × 6), and the spatial arrangement of the two test lights (parallel or diagonal) were compared (Supplementary Figs. S1a–d). In these pilot experiments, blue (λmax = 470 nm) and green (λmax = 526 nm) lights were used for evaluation (Supplementary Fig. S1f). Among the tested conditions, the protocol employing 36˚C as the aversive temperature, one-minute training repeated six times, and diagonally arranged test lights produced robust discrimination (LI = 0.132 ± 0.040

	combinations	mean PI	SEM	n	p value	$p < \alpha$
1	V_{100} vs. V_{10}	-0.0392	0.040	20	3.35.E-01	n.s.
2	B_{100} vs. B_{10}	-0.0873	0.040	20	5.93.E-02†	n.s.
3	G_{100} vs. G_{10}	-0.0498	0.050	20	3.31.E-01	n.s.
4	Y_{100} vs. Y_{10}	0.0918	0.038	20	2.74.E-02	n.s.
5	O_{100} vs. O_{10}	0.0749	0.026	20	1.03.E-02	n.s.
6	R_{100} vs. R_{10}	0.0406	0.040	20	3.27.E-01	n.s.

Table 2. Preference index (PI) for spectral preference between different intensities of each LED color. V, violet; B, blue; G, green; Y, yellow; O, orange; R, red; PI, preference index. One sample t-tests were used to assess differences from zero; statistical significance is indicated by asterisks (*) for $p < 0.05$ after Bonferroni correction (adjusted $\alpha = 0.0083$) †Wilcoxon signed-rank tests were used when data violated the assumption of normality (Shapiro-Wilk test).

(mean ± SEM), $n = 14$, $p = 2.32.E-03$; Supplementary Figs. S1c, d, statistical details are provided in Supplementary Tables S2,S3), and was thus selected as the standard procedure. Under these conditions, a control experiment in which the aversive stimulus was replaced with 22°C yielded an LI value of $0.0056 ± 0.023$ ($n = 14$, $p = 0.815$; Supplementary Figs. S1c, d, statistical details are provided in Supplementary Table S3), indicating that aversive temperature and/or relief from aversive temperature induce learning.

Since color vision is defined as the ability to discriminate between two different wavelengths independent of their intensity, we tested whether our experimental conditions satisfy this criterion. We employed conversion experiments[19,41] in which the intensities of the lights are inverted between conditioning and testing phases; flies were conditioned with 100% bright blue vs. 10% dark green and tested with 100% bright green vs. 10% dark blue, or vice versa. Flies did not show significant discrimination (when trained with 100% blue vs. 10% green, LI = $0.0501 ± 0.059$, $n = 14$, $p = 4.11.E-01$; when trained with 10% blue vs. 100% green, LI = $-0.0490 ± 0.042$, $n = 14$, $p = 2.61.E-01$; Supplementary Fig. S1e, statistical details are provided in Supplementary Table S4). Next, we tested 1:2 intensity ratio intensity difference (100% vs. 50%) between the conditioning and testing, and flies successfully discriminated in this case (when trained with 100% blue vs. 50% green, LI = $0.1245 ± 0.040$; $n = 14$, $p = 8.10.E-03$; when trained with 50% blue vs. 100% green, LI = $0.1165 ± 0.031$, $n = 14$, $p = 2.42.E-03$; Supplementary Fig. S1e, statistical details are provided in Supplementary Table S4). These results suggest that flies can learn to discriminate blue vs. green based on wavelength to some extent, although contributions from intensity differences cannot be entirely excluded in this assay.

Discrimination between different wavelength and intensity combinations

Next, we examined the flies' ability to discriminate between different wavelength combinations across a wide spectral range using our behavioral system (Fig. 1e). Significant discrimination was observed for combinations of violet vs. blue (LI = $0.116 ± 0.019$ (mean ± SEM), $n = 30$, $p = 9.54.E-07$, statistical details are provided in Table 3), violet vs. green (LI = $0.102 ± 0.026$, $n = 30$, $p = 4.53.E-04$), and blue vs. green (LI = $0.093 ± 0.020$, $n = 30$, $p = 5.24.E-05$), whereas green, yellow, orange, and red were not discriminated from one another (green vs. yellow, LI = $-0.010 ± 0.042$, $n = 26$, $p = 8.16.E-01$; green vs. orange, LI = $0.024 ± 0.032$, $n = 26$, $p = 4.55.E-01$; green vs. red, LI = $0.011 ± 0.029$, $n = 26$, $p = 7.20.E-01$; yellow vs. orange, LI = $0.029 ± 0.026$, $n = 26$, $p = 2.83.E-01$; yellow vs. red, LI = $-0.003 ± 0.024$, $n = 26$, $p = 8.91.E-01$; orange vs. red, LI = $0.019 ± 0.030$, $n = 26$, $p = 5.42.E-01$; Fig. 3a, statistical details are provided in Table 3). Combinations of shorter wavelengths (violet and blue) with longer wavelengths (yellow, orange, and red) showed moderate LIs, although these were not statistically significant (violet vs. yellow, LI = $0.049 ± 0.028$, $n = 26$, $p = 9.07.E-02$; violet vs. orange, LI = $0.053 ± 0.036$, $n = 26$, $p = 1.49.E-01$; violet vs. red, LI = $0.041 ± 0.035$, $n = 26$, $p = 7.34.E-02$; blue vs. yellow, LI = $0.049 ± 0.033$, $n = 30$, $p = 1.51.E-01$; blue vs. orange, LI = $0.092 ± 0.036$, $n = 30$, $p = 1.62.E-02$; blue vs. red, LI = $0.051 ± 0.035$, $n = 30$, $p = 1.52.E-01$; Fig. 3a, statistical details are provided in Table 3). These results suggest that flies can discriminate between short to middle wavelengths (violet to green), but not between middle to long wavelengths (green to red). Since we could not rule out the possibility that discrimination was based on differences in light intensity, we next tested discrimination of intensity differences at each individual wavelength.
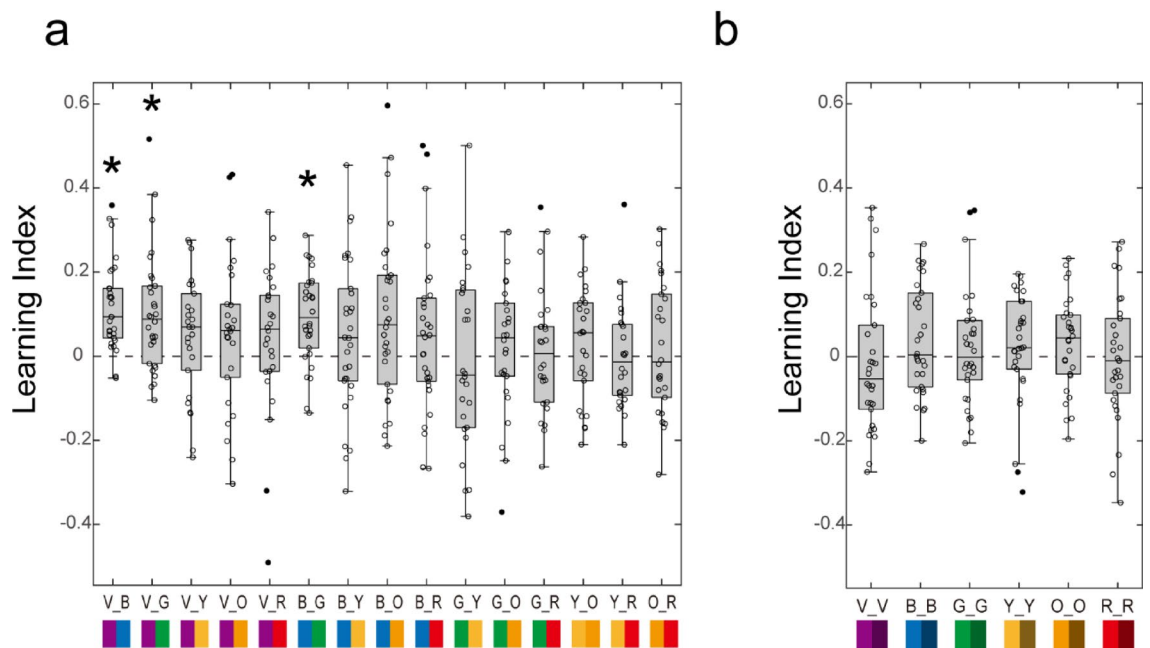
We tested the ability to discriminate luminance differences (100% vs. 10%; light intensities shown in Figs. 1e, f) for all six monochromatic light wavelengths. Flies showed no significant discrimination at any wavelength (violet 100% vs. 10%, LI = $-0.0169 ± 0.030$, $n = 30$, $p = 5.84.E-01$; blue 100% vs. 10%, LI = $0.0399 ± 0.024$, $n = 30$, $p = 1.78.E-01$; green 100% vs. 10%, LI = $0.0187 ± 0.025$, $n = 30$, $p = 4.61.E-01$; yellow 100% vs. 10%, LI = $0.0196 ± 0.024$, $n = 30$, $p = 4.27.E-01$; orange 100% vs. 10%, LI = $0.0330 ± 0.020$, $n = 30$, $p = 1.12.E-01$; red 100% vs. 10%, LI = $-0.0049 ± 0.027$, $n = 30$, $p = 8.58.E-01$; Fig. 3b, statistical details are provided in Table 4), indicating that the observed discrimination behavior was based primarily, if not entirely, on spectral information.

Comparison of behavioral results with photoreceptor space representation

Once the spectral sensitivities of a species are known, the quantum catch of each photoreceptor in response to a given light stimulus can be calculated (Figs. 4a, b). Here, we compared our behavioral results with the categorical model proposed by Troje[18]. According to the model, stimuli plotted in different categories (quadrants) of this photoreceptor space can be discriminated, whereas those within the same category cannot. In our case, all six

	combinations	mean LI	SEM	n	p value	p < α
1	V vs. B	0.116	0.019	30	9.54.E-07	*
2	V vs. G	0.102	0.026	30	4.53.E-04†	*
3	V vs. Y	0.049	0.028	26	9.07.E-02	n.s
4	V vs. O	0.053	0.036	26	1.49.E-01	n.s
5	V vs. R	0.041	0.035	26	7.34.E-02†	n.s
6	B vs. G	0.093	0.020	30	5.24.E-05	*
7	B vs. Y	0.049	0.033	30	1.51.E-01	n.s
8	B vs. O	0.092	0.036	30	1.62.E-02	n.s
9	B vs. R	0.051	0.035	30	1.52.E-01	n.s
10	G vs. Y	-0.010	0.042	26	8.16.E-01	n.s
11	G vs. O	0.024	0.032	26	4.55.E-01	n.s
12	G vs. R	0.011	0.029	26	7.20.E-01	n.s
13	Y vs. O	0.029	0.026	26	2.83.E-01	n.s
14	Y vs. R	-0.003	0.024	26	8.91.E-01	n.s
15	O vs. R	0.019	0.030	26	5.42.E-01	n.s

Table 3. Learning index (LI) for discrimination between pairs of six LED colors. V, violet; B, blue; G, green; Y, yellow; O, orange; R, red; LI, learning index. One sample t-tests were used to assess differences from zero; statistical significance is indicated by asterisks (*) for $p < 0.05$ after Bonferroni correction (adjusted $\alpha = 0.0033$) †Wilcoxon signed-rank tests were used when data violated the assumption of normality (Shapiro-Wilk test).
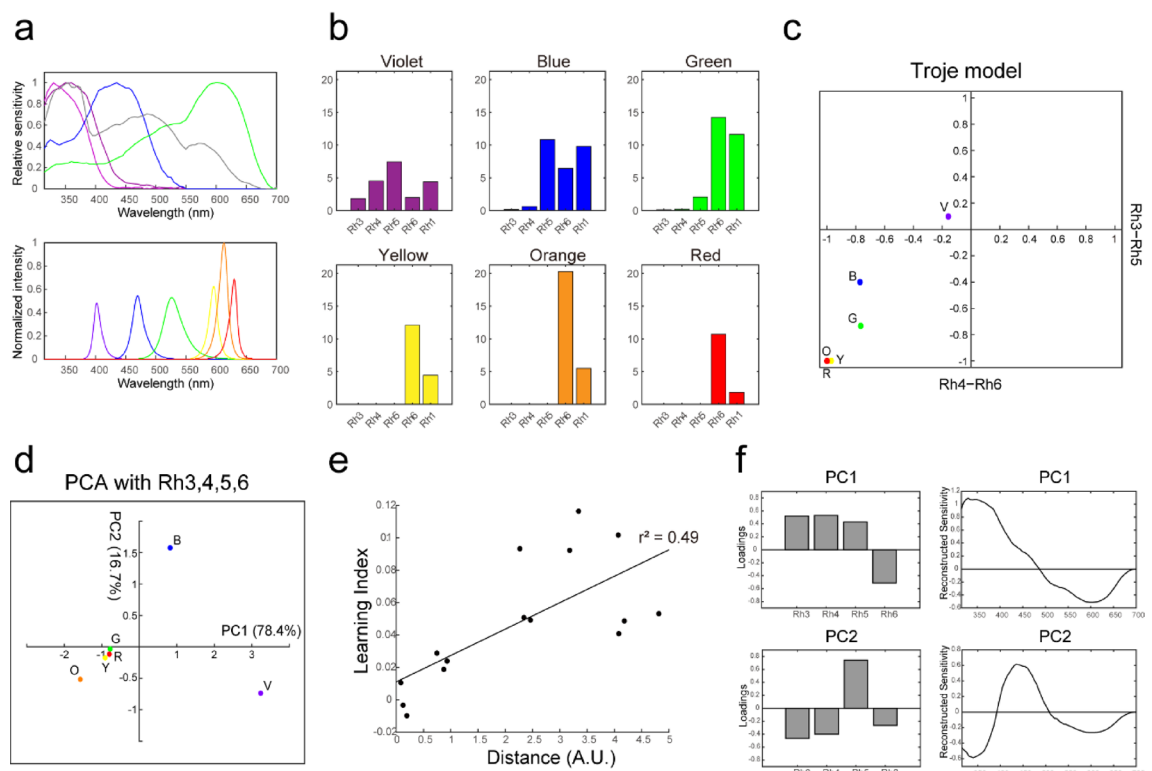

Fig. 3. Learning discrimination for combinations of six monochromatic lights. **a.** Learning discrimination for each combination of six monochromatic LEDs (violet, blue, green, yellow, orange, and red) ($n = 26$–30). **b.** Learning discrimination for intensity differences in six monochromatic wavelengths ($n = 30$). The intensity difference is approximately 1:10 (see Figs. 1e, f). Statistically significant differences from zero were assessed with a one sample t-test or a Wilcoxon signed-rank test. *$p < 0.05$, after p-values were Bonferroni corrected. Mean values and other statistical information are summarized in Tables 3 and 4.

light stimuli except violet were plotted in the bottom-left quadrant, while violet appeared in the upper-left quadrant, suggesting that this model does not account for our behavioral results (Fig. 4c, see also Discussion).

Due to difficulties in applying conventional models to explain the discrimination observed in our data, we adopted a more straightforward representation of each color stimulus in photoreceptor space, where each axis corresponds to the quantum catch of a specific photoreceptor. The distance between points in this space serves as an estimate of the discriminability between two stimuli. Because the sensitivities of the photoreceptors are highly correlated, we applied principal component analysis (PCA) using four photoreceptors (Rh3, Rh4, Rh5,

	combinations	mean LI	SEM	n	p value	$p < \alpha$
1	V_{100} vs. V_{10}	-0.0169	0.030	30	5.84.E-01	n.s
2	B_{100} vs. B_{10}	0.0399	0.024	30	1.78.E-01†	n.s
3	G_{100} vs. G_{10}	0.0187	0.025	30	4.61.E-01	n.s
4	Y_{100} vs. Y_{10}	0.0196	0.024	30	4.27.E-01	n.s
5	O_{100} vs. O_{10}	0.0330	0.020	30	1.12.E-01	n.s
6	R_{100} vs. R_{10}	-0.0049	0.027	30	8.58.E-01	n.s

Table 4. Learning index (LI) of discrimination between different intensities of each LED color. V, violet; B, blue; G, green; Y, yellow; O, orange; R, red; LI, learning index. One sample t-tests were used to assess differences from zero; statistical significance is indicated by asterisks (*) for $p < 0.05$ after Bonferroni correction (adjusted $\alpha = 0.0083$) †Wilcoxon signed-rank tests were used when data violated the assumption of normality (Shapiro-Wilk test).

Fig. 4. Comparison of the color representation in the photoreceptor space and the behavioral results. **a**. Spectral sensitivity of the photoreceptors reported in Sharkey et al. 2020[15] (upper) and spectra of the LED lights used in the learning experiments (bottom). The quantum catch for each photoreceptor was calculated by multiplying its spectral sensitivity by the LED light spectrum and integrating the product over the range of 315 to 700 nm (see Methods). **b**. Calculated quantum catch for each LED light. **c**. Light stimuli are represented on the map of Troje's categorical model[18]. **d**. Principal component analyses for the six LED colors based on the calculated quantum catches of the four photoreceptors: Rh3, Rh4, Rh5, and Rh6. The percentages of variance accounted by the PC1 and PC2 are shown on each axis. **e**. Correlations between the pairwise distances between each color represented in the PC1 and PC2 space and the mean learning indices in the aversive visual learning. **f**. Loadings of the PC1 (upper left) and PC2 (bottom left). Reconstructed sensitivities of the PC1 (upper right) and PC2 (bottom right).

and Rh6) to efficiently represent the photoreceptor space. Each color stimulus was then mapped onto a two-dimensional space defined by the first two principal components, PC1 and PC2, which together explain over 95% of the total variance (78.4% for PC1 and 16.7% for PC2; Fig. 4d). We further compared the distances between these color loci with the mean learning indices (LIs) obtained from learning discrimination experiments (Fig. 4e). This representation predicted behavioral discrimination reasonably well ($r^2 = 0.49$), capturing the discriminability among violet, blue and green, as well as the lack of discrimination among green, yellow, orange, and red. Moreover, this correlation was stronger than that obtained using the photoreceptor space defined by all

photoreceptors, including Rh1 (r^2 = 0.30; Supplementary Fig. S3). Finally, by multiplying the PCA loadings by the spectral sensitivities of each photoreceptor, we reconstructed the sensitivities of the two axes, revealing two opponent channels: short (Rh3 and Rh4) vs. long (Rh6) for PC1, and middle (Rh5) vs. short (Rh3 and Rh4) plus long (Rh6) for PC2 (Fig. 4f).

Discussion

We conducted a spectral preference assay and a visual learning assay using heat as an aversive stimulus to evaluate the flies' ability to discriminate between various combinations of wavelengths and light intensities. We then compared our behavioral results with existing coding models by incorporating the spectral sensitivities of individual photoreceptors and estimated each photoreceptor's contribution to color discrimination.

A caveat of this study concerns the choice of *Drosophila* strain. We used the wild-type Canton-S line as a representative of *D. melanogaster*. However, previous reports have shown that phototactic behavior can vary depending on the strain[47,48]. In fact, one of the original study on phototaxis deliberately selected the Canton-S line because of its strong light response[47]. Thus, our findings may not be fully generalizable to other *D. melanogaster* strains. Although several studies have reported that Canton-S and other wild-type strains exhibit comparable phototactic and spectral preference behaviors[34,36] it remains possible that spectral preference is influenced by genetic background. Moreover, previous research has shown that phototactic behavior can also be affected by individual variation[48]. Therefore, both genetic and environmental factors may influence innate spectral preference, and similar considerations should be applied when interpreting learned chromatic behaviors.

In our slow phototactic assay, flies exhibited an innate preference for moderately longer wavelengths (green to orange) and avoidance of shorter wavelengths (violet to blue), contrasting with the short-wavelength preference seen in fast phototaxis. Similar findings include a green preference over blue in *D. melanogaster*[49] and an innate preference for yellow wavelengths in some dipteran species, such as the blow fly[50] and the hover fly *Eristalis tenax*[51]. These results suggest that yellow to orange wavelengths may have an innate attractive effect in some dipteran species, although the underlying neural mechanisms and ecological significance remain unclear[11]. Conversely, shorter wavelengths can be harmful to flies[52,53]. A recent study demonstrated consistent blue avoidance mediated by Rh7 and the TRP channel Painless in neurons located on the body surface at high light intensities[29]. This study also shows that the green preference at dawn and dusk is mediated by Rh1 receptors and dynamically modulated by the circadian rhythm through the action of the TRP channels, TrpA1 and Pyrexia. Although the behavioral contexts differ and thus direct comparison to our study is limited, the blue avoidance observed here may also be mediated by a non-visual component, while the green preference may be mediated by Rh1 receptors. Additionally, extraretinal photosensitive molecules such as cryptochrome and Rh7 have been shown to influence the activity levels of flies[21,24,54,55]. Further research is needed to identify the photoreceptor inputs and other extraretinal photosensitive components involved in slow phototactic behaviors, using genetic manipulations of candidate photoreceptors and extraretinal photosensitive molecules, as well as analyses of downstream circuit elements.

In this study, we introduced a newly developed visual learning assay. Various types of associative visual learning assays have been established for flies[18,19,41,43–45,50,56] differing in factors such as the number of flies tested (individuals or groups), the type of unconditioned stimulus used (appetitive stimuli like sucrose as a reward or aversive stimuli such as electric shock, shaking, or heat as punishment), and the conditioning method applied (differential or absolute). Our assay was designed based on the behavioral paradigm developed by Schnaitmann et al., who demonstrated blue vs. green color discrimination using appetitive learning with sucrose reward[19,49]. We also referred to Spatz et al.'s work, which evaluated color discrimination starting with blue vs. yellow, followed by various other color combinations, using aversive learning with shaking punishment[41,42].

Like these assays, our method uses a population of flies freely walking in an illuminated arena during both conditioning and testing. Population-based assays offer a practical approach and can reduce variability between individuals, though group effects may still influence results[57]. We employed aversive heat as the unconditioned stimulus, a stimulus well-established in conventional single-fly assays using infrared beams[43,44]. Finally, differential conditioning was applied in our assay; this method has been shown to enhance color discrimination in honeybees[58]. While we assume the heat stimulus induces aversion, relief from the aversive temperature may also act as positive reinforcement.

There are several potential limitations in our study that should be acknowledged. First, our visual learning assay did not conclusively demonstrate that flies discriminated between two visual cues based solely on wavelength differences, independent of light intensity. Rather, we showed that flies were unable to discriminate intensity differences at each wavelength but could distinguish between several wavelength combinations with relatively small intensity differences. To accurately separate the contributions of wavelength and intensity, it is essential to assess the animal's perception of subjective brightness. However, currently, no established behavioral paradigm exists to fully disentangle these two factors in insects[9]. An alternative approach is the conversion experiment, which in our study showed moderate discriminability based on wavelength over intensity (Supplementary Fig. S1e). Second, our assay evaluated flies' preference for direct light emitted from the light source, rather than for object colors reflected under illumination. Although this method allows greater control over wavelength and intensity of the stimuli and is commonly used with the assumption that the perceived sensation corresponds to object color detection (e.g. [18,19,42,59]), there remains a caveat regarding potential photoreceptor adaptation[11]. Third, as described above, some TRP channels may be sensitive to both light and temperature and could play a role in spectral preference behavior[29]. These TRP channels may be influenced by both the light stimuli and the aversive heat stimuli used in our learning paradigm; however, their actual contribution was not examined in this study. Finally, the learning scores in our assay were relatively low even when flies significantly discriminated between two colors. In general, visual learning in *D. melanogaster* tends to show lower performance compared to olfactory learning, regardless of the type of unconditioned stimulus employed[39]. This likely reflects an inherent

bias in *D. melanogaster's* learning abilities toward olfactory cues, possibly related to the relative amount of neural input to the mushroom body[60,61].

Our results showed that flies could discriminate combinations of violet, blue, and green wavelengths, but could not discriminate combinations involving green, yellow, orange, and red. This suggests that discriminability is enhanced in the wavelength range where the spectral sensitivities of multiple photoreceptors overlap, rather than in regions where their sensitivities do not overlap. Most previous studies on color vision in *D. melanogaster* have focused on blue vs. yellow[40,41] or blue vs. green[19,43,44] with only one study examining a relatively wide spectral range[42]. Therefore, our study provides a second piece of evidence regarding spectral discrimination properties in *D. melanogaster*, under different behavioral conditions, offering valuable insights into the spectral discrimination abilities of this important model organism. Our findings contrast with those of Salomon et al. (1983)[42] as flies in our study showed weak discriminability between middle (green) to longer (red) wavelengths, indicating that wavelength dependency in learning may vary across the entire visible spectrum. Similar results have been reported in other fly species, where discrimination at green and red wavelengths is less robust compared to blue and yellow[50]. This reduced wavelength contrast may be due to a lack of variation in long-wavelength photoreceptors in flies. A similar trait is observed in bees, which possess three classes of spectrally sensitive photoreceptors, with peak sensitivities in the ultraviolet, blue, and green ranges[62] and exhibit poor red discrimination[63]. In contrast, butterflies have greater photoreceptor variation from duplications and screening pigments, including red receptors sensitive to longer wavelengths[64,65] enabling them to achieve fine discrimination in this range[66,67]. Whether the use of photoreceptors is conserved across insect species or is species-specific remains a matter of debate[13,68–70].

Although our results showed that flies were unable to learn to discriminate based on intensity differences, the potential influence of intensity differences cannot be entirely ruled out. Previous studies have demonstrated that flies are capable of learning to distinguish differences in light intensity under certain conditions[19,45,46]. However, it has also been shown that chromatic information tends to be prioritized over intensity cues, as well as over other achromatic cues such as form[19,41,44] suggesting that chromatic cues may be a more salient visual feature for flies in these behavioral contexts. Similarly, in our experiments, wavelength differences may have been perceived as more salient than intensity differences. In contrast, honeybees have been shown to use chromatic and achromatic information differently depending on visual angle: achromatic contrast is used for objects subtending 5–15˚ of visual angle, while chromatic contrast is used for objects larger than 15˚[71,72]. The neural mechanisms underlying such context-dependent visual processing in honeybees—and whether similar strategies are employed by *Drosophila*—remain unclear.

Modeling approaches that incorporate photoreceptor spectral sensitivities and behavioral data are commonly used to predict which photoreceptors contribute to color discrimination[1]. Regarding color discrimination in Diptera, an influential model proposed categorical discrimination in the blow fly[18]. This model has been supported by studies in other fly species[73] and widely used to represent dipteran color space (e.g.[74–76]). However, our results do not align with this model, as blue, green, yellow, orange, and red stimuli all fall within the same category (Fig. 4c). This discrepancy may be partly due to experimental conditions. Our assays were conducted in darkness, without accounting for photoreceptor adaptation to background light. Troje's original model, by contrast, included gain adjustments based on light adaptation and defined four categories: UV, blue, green, and purple (UV–green). Applying similar gain adjustments to our data, the resulting map aligned more closely with our behavioral data, though only marginally (Supplementary Fig. S2). Additional experiments using a broader set of wavelength combinations—both within and across the proposed categories—are necessary to further evaluate the validity of this model.

We also considered applying the receptor noise-limited (RNL) color-opponent model, another widely used framework for insect color vision[77]. This model allows for the calculation of a spectral discrimination function ($\Delta\lambda$), which can be compared with behavioral data[59]. However, the limited number of wavelengths tested in our behavioral experiments prevented an accurate reconstruction of the spectral discrimination function. Therefore, we conclude that our dataset is not suitable for applying the RNL model.

We evaluated the distances between monochromatic light stimuli in photoreceptor space, defined by the quantum catches of each photoreceptor, and compared models with and without the broadband Rh1 photoreceptor. To reduce redundancy among photoreceptor spectral sensitivities, we applied PCA, representing color loci in a two-dimensional space defined by PC1 and PC2. The model excluding Rh1 provided a better fit to our behavioral data, consistent with previous proposals that Rh1 does not substantially contribute to chromatic processing in flies[18,78]. This finding contrasts with prior models suggesting that inclusion of Rh1 improves alignment with behavioral outcomes[19,79]. Notably, inclusion of Rh1 in our model resulted in a clear separation of green from longer wavelengths (yellow, orange, and red), which was not supported by our behavioral observations (Supplementary Fig. S3a). To further examine the nature of photoreceptor interactions underlying color discrimination, we reconstructed the PC1 and PC2 axes (Fig. 4f). The resulting opponent axes closely resembled those described by Heath et al.[78], indicating that similar chromatic processing mechanisms may be conserved. Nonetheless, discrepancies between the model and empirical data persist. In particular, while the model predicted large perceptual distances between violet and longer wavelengths, behavioral discrimination in this range was limited. This suggests that additional factors—such as perceptual brightness or context-dependent sensitivity—may influence color discrimination and should be considered in future models. In addition, our study did not include light stimuli in the UV range, which may have reduced the contribution of photoreceptors sensitive to these wavelengths.

Here, we characterized both innate spectral preferences and learned chromatic discrimination in *D. melanogaster* using a defined behavioral paradigm. While the neural circuits linking photoreceptor input to chromatic behavior remain largely unresolved across insect taxa, recent studies in *D. melanogaster* have elucidated mechanisms of color opponency mediated by inhibitory interactions among photoreceptor axons[78,80]. Although

color-opponent neurons in higher brain centers remain elusive[60,81] recent studies have identified circuits within the optic lobe that involve interactions between chromatic and achromatic pathways, as well as color-opponent neurons exhibiting spatially and spectrally double-opponent properties[82–84]. These findings, together with the uniquely detailed connectomic datasets now available for *D. melanogaster*[85] set the stage for comprehensive circuit-level analysis of spectral coding. Our behavioral results provide foundational data to support such efforts. By refining the current paradigm and combining the powerful genetic tools, future studies are well positioned to resolve the neural computations underlying spectral processing at single-cell resolution—an objective that remains difficult to achieve in other systems.

Materials and methods

Fly stocks
All flies were maintained on conventional cornmeal agar medium under a 12-hour light: 12-hour dark cycle at 24 ˚C. Flies 3 – 10 days after eclosion were used in all experiments. The fly line used in this study was the wild-type strain Canton-S, which was provided by Dr. A. Nose.

Fly chamber
Flies were placed in a custom-made acrylic chamber produced using a 3D printer (DMM.make, https://make.dmm.com/). The chamber size was $55 \times 75 \times 20$ mm, with a sliding slit through which two thin plastic plates were inserted. An acrylic plate ($55 \times 75 \times 1$ mm) was attached to the bottom of the chamber using adhesive. Approximately 50 flies were transferred into the chamber using an aspirator through a small hole in the plastic plate. Afterward, the hole was covered with another plastic plate. The space available for the flies to move freely was $55 \times 75 \times 3$ mm. Males and females were not distinguished. The chamber was cleaned with wet paper soaked in distilled water after each experiment and thoroughly washed at the end of each experimental day.

Experimental apparatus
Two sets of conditioning apparatus (Fig. 1c) and two sets of testing apparatus (Fig. 1d) were placed side by side in a darkroom. A conditioning apparatus consisted of electric circuits built on a breadboard that controlled illumination from light-emitting diodes (LEDs) and a cooling plate that regulated temperature (Fig. 1c). Six wavelengths of LEDs (all sourced from AKIZUKI DENSHI TSUSHO CO., LTD) were used: violet (OSV5YL3131A, λ_{max} = 402 nm), blue (OSB56A3131A, λ_{max} = 470 nm), green (OSPG3131P, λ_{max} = 526 nm), yellow (OS5YKA3131A, λ_{max} = 596 nm), orange (OS5OAA3131A, λ_{max} = 613 nm), and red (OS5RKA3131P, λ_{max} = 630 nm). The wavelengths and intensities of the light were measured using a spectrometer (HSU-100S, Asahi Spectra) (Figs. 1e, f). The LED circuits consisted of four units, with each unit containing five 3-mm LEDs connected in series. Each LED was covered with a diffusion cap. The four sections of the chamber were illuminated by each LED unit through the separator. The black nylon separator, produced using a 3D printer (DMM.make), measured $55 \times 75 \times 50$ mm with the four sections separated by thin walls. The top of the separator was covered with a sheet of paper. The light intensity was adjusted using carbon resistors, and electric power was supplied to each unit by a 24 V AC adapter. For conditioning, LEDs of the same wavelengths were mounted in each of the four units, and the chamber was illuminated from above. A testing apparatus consisted of the same electrical circuits that controlled illumination as the conditioning chamber (Fig. 1D). For testing, LEDs of two different wavelengths were mounted diagonally (or parallel in the pilot experiments), and the chamber was placed on the separator and illuminated from below.

Preference experiments
Preferences for the two light stimuli were evaluated using the test apparatus without conditioning. Flies were housed in the chamber, and after a two-minute dark-adaptation period, five-minute tests were conducted and recorded using a CMOS camera (DCC1545M, Thorlabs) positioned above. During the tests, the flies moved freely within the chamber, which was illuminated by two light stimuli projected diagonally opposite each other. The number of flies distributed after two minutes was counted, and preference indices were calculated.

Discrimination experiments
We employed classical associative learning with differential conditioning using aversive temperature as the unconditioned stimulus (US) and light from LEDs as the conditioned stimulus (CS). During the training phase, the chamber was placed in the conditioning apparatus and positioned on the cooling plate, where the temperature inside the chamber was set to either an aversive level (34,36, or 39˚C) or a normal level (22˚C). Light from LEDs was projected onto the chamber from above through the separator. Two sets of conditioning apparatus were placed symmetrically, with one set configured to an aversive temperature associated with one light stimulus and the other set configured to normal temperature associated with the other stimulus. After the fixed training period (the standard protocol was one minute), the two chambers were swapped, and the flies were trained under the other condition for an additional period (Supplementary Figs. S1a, c). This procedure was repeated several times (the standard protocol was six times). After approximately 30 s in a dark place at room temperature, the chamber was moved to the test apparatus. During the tests, the flies moved freely within the chamber, which was illuminated by two light stimuli projected diagonally opposite each other (or in parallel during pilot experiments). Then, five-minute tests were conducted and recorded using a CMOS camera positioned above. The number of flies distributed after two minutes was counted, and learning indices were calculated. The tests were performed at room temperature.

Preference and learning indices

The number of flies after two minutes was counted. A preference index (PI) for wavelength λ_A vs. wavelength λ_B was calculated as the difference between the number of flies in area A, illuminated by wavelength λ_A, minus the number of flies in area B, illuminated by wavelength λ_B, divided by the total number of flies:

$$PI = (\#\text{flies in A} - \#\text{flies in B})/(\#\text{flies in A} + \#\text{flies in B})$$

For the discrimination experiments, preference indices for pattern I (PI_1), where wavelength λ_A was associated with the aversive temperature and wavelength λ_B was associated with the normal temperature, and for pattern II (PI_2), where wavelength λ_B was associated with the aversive temperature and wavelength λ_A was associated with the normal temperature, were calculated first for each experiment as above:

$$PI_1 = (\#\text{flies in B} - \#\text{flies in A})/(\#\text{flies in B} + \#\text{flies in A})$$

$$PI_2 = (\#\text{flies in A} - \#\text{flies in B})/(\#\text{flies in A} + \#\text{flies in B})$$

Then, a learning index (LI) was calculated for the two consecutive experiments as follows:

$$LI = (PI_1 + PI_2)/2$$

The preference indices (PIs) from the two patterns of differential experiments were averaged. The LI indicated how well the flies learn to discriminate between two visual stimuli, with values ranging from 1 to -1. A value of 1 indicates that all flies chose the light associated with the normal temperature, 0 indicates a neutral response, and -1 indicates all flies chose the light stimulus associated with the aversive temperature. The LI canceled out the innate preference for one of the stimuli, which was assumed to be symmetrically overlaid in both patterns of preference indices.

Visual models

Relative spectral sensitivity of each photoreceptor (Rh1, Rh3, Rh4, Rh5, and Rh6) was obtained from a recent study, where photoreceptor sensitivities were measured in vivo[15].

The quantum catch for photoreceptor i was calculated as follows:

$$Q_i = \int_{315}^{700} I(\lambda) * S_i(\lambda)\ d\lambda$$

Where $I(\lambda)$ was the normalized light intensity of a light stimulus and $S_i(\lambda)$ is the spectral sensitivity of the i-th receptor. Based on the quantum catch of each photoreceptor, the visual stimulus was plotted in photoreceptor space.

Troje's categorical models

The categorical color vision model was proposed by Troje[18]. Based on the quantum catch values Q_i calculated above, photoreceptor excitations were computed as follows:

$$E_i = Q_i / (Q_i + 1)$$

Where E_i can take any value between 0 and 1. The categorical model consists of two axes of inner photoreceptor subtractions in either pale-type or yellow-type ommatidia; $p = (E_3 - E_5) / (E_3 + E_5)$, $y = (E_4 - E_6) / (E_4 + E_6)$. If the stimulus spectrum did not overlap with the spectral sensitivity of the photoreceptors defined for each axis, -1 or 1 was assigned, depending on whether the stimulus wavelength was shifted to longer or shorter wavelength, respectively. Achromatic information was excluded. There are four categories depending on the polarity of the subtractions of these inner photoreceptors: $p-y-$, $p-y+$, $p+y+$, and $p+y-$.

Representation in photoreceptor space via dimensionality reduction

Quantum catches of each photoreceptor for each LED stimulus were calculated, and the LED stimuli were represented as four-dimensional or five-dimensional vectors. Principal component analysis (PCA) was applied to the quantum catches of the six LED stimuli (violet, blue, green, yellow, orange, and red) across the four photoreceptors (Rh3–Rh6) or the five photoreceptors (Rh3–Rh6 and Rh1). The quantum catch values were transformed to z-score before PCA to normalize the weights of each photoreceptor. Each LED stimulus was then plotted in a two-dimensional space, with PC1 and PC2 as the axes. The distances between the six LED stimuli were calculated using the Euclidean distance metric. Linear regression analyses were performed between the distances in photoreceptor space and the mean values of LI.

Statistics

Statistical analyses were performed using MATLAB software with the Statistics and Machine Learning Toolbox (MathWorks). For the spectral preference and learning discrimination experiments, if the data did not violate the assumption of normality (Shapiro-Wilk test), statistically significant differences from zero were assessed using a one-sample t-test with a Bonferroni correction. If the data significantly deviated from the assumption of normality, Wilcoxon signed-rank tests with a Bonferroni correction were applied. Statistical details are presented

in Tables 1, 2 and 3 and Tables S2–S4, including the specific statistical tests applied to each dataset. All the graphs are presented as boxplots, which display the median (central line) and quartiles (boxes), with the whiskers extending to the minimum and maximum points within 1.5 times the interquartile range. Individual value plots are overlaid onto the boxplots.

Data availability

References

1. Kelber, A., Vorobyev, M. & Osorio, D. Animal colour vision – behavioural tests and physiological concepts. *Biol. Rev. Camb. Philos. Soc.* **78**, 81–118. https://doi.org/10.1017/s1464793102005985 (2003).
2. Osorio, D. & Vorobyev, M. Photoreceptor spectral sensitivities in terrestrial animals: adaptations for luminance and colour vision. *Proceedings. Biological sciences / The Royal Society* **272**, 1745–1752, (2005). https://doi.org/10.1098/rspb.2005.3156
3. van Hateren, J. H. Spatial, Temporal and spectral pre-processing for colour vision. *Proc. Biol. Sci.* **251**, 61–68. https://doi.org/10.1098/rspb.1993.0009 (1993).
4. Osorio, D. & Vorobyev, M. A review of the evolution of animal colour vision and visual communication signals. *Vision. Res.* **48**, 2042–2051. https://doi.org/10.1016/j.visres.2008.06.018 (2008).
5. Gegenfurtner, K. R. & Kiper, D. C. Color vision. *Annu. Rev. Neurosci.* **26**, 181–206. https://doi.org/10.1146/annurev.neuro.26.041002.131116 (2003).
6. Kelber, A. & Osorio, D. From spectral information to animal colour vision: experiments and concepts. *Proc. Biol. Sci.* **277**, 1617–1625. https://doi.org/10.1098/rspb.2009.2118 (2010).
7. Song, B. M. & Lee, C. H. Toward a mechanistic Understanding of color vision in insects. *Front. Neural Circuits.* **12** https://doi.org/10.3389/fncir.2018.00016 (2018).
8. Behnia, R. & Desplan, C. Visual circuits in flies: beginning to see the whole picture. *Curr. Opin. Neurobiol.* **34**, 125–132. https://doi.org/10.1016/j.conb.2015.03.010 (2015).
9. Schnaitmann, C., Pagni, M. & Reiff, D. F. Color vision in insects: insights from *Drosophila*. *J. Comp. Physiol. A. Neuroethol. Sens. Neural. Behav. Physiol.* **206**, 183–198. https://doi.org/10.1007/s00359-019-01397-3 (2020).
10. Currier, T. A., Pang, M. M. & Clandinin, T. R. Visual processing in the fly, from photoreceptors to behavior. *Genetics* **224** https://doi.org/10.1093/genetics/iyad064 (2023).
11. Lunau, K. Visual ecology of flies with particular reference to colour vision and colour preferences. *J. Comp. Physiol. A. Neuroethol. Sens. Neural. Behav. Physiol.* **200**, 497–512. https://doi.org/10.1007/s00359-014-0895-1 (2014).
12. Hardie, R. C. The photoreceptor array of the dipteran retina. *Trends Neurosci.* **9**, 419–423 (1986).
13. Wernet, M. F., Perry, M. W. & Desplan, C. The evolutionary diversity of insect retinal mosaics: common design principles and emerging molecular logic. *Trends Genet.* **31**, 316–328. https://doi.org/10.1016/j.tig.2015.04.006 (2015).
14. Salcedo, E. et al. Blue- and green-absorbing visual pigments of *Drosophila*: ectopic expression and physiological characterization of the R8 photoreceptor cell-specific Rh5 and Rh6 rhodopsins. *J. Neuroscience: Official J. Soc. Neurosci.* **19**, 10716–10726 (1999).
15. Sharkey, C. R., Blanco, J., Leibowitz, M. M., Pinto-Benito, D. & Wardill, T. J. The spectral sensitivity of *Drosophila* photoreceptors. *Sci. Rep.* **10**, 18242. https://doi.org/10.1038/s41598-020-74742-1 (2020).
16. Wernet, M. F. et al. Homothorax switches function of *Drosophila* photoreceptors from color to polarized light sensors. *Cell* **115**, 267–279 (2003).
17. Mazzoni, E. O. et al. Iroquois complex genes induce co-expression of rhodopsins in *Drosophila*. *PLoS Biol.* **6**, e97. https://doi.org/10.1371/journal.pbio.0060097 (2008).
18. Troje, N. Spectral categories in the learning behaviour of blowflies. *Z. Für Naturforschung C.* **48**, 96–104 (1993).
19. Schnaitmann, C., Garbers, C., Wachtler, T. & Tanimoto, H. Color discrimination with broadband photoreceptors. *Curr. Biology: CB.* **23**, 2375–2382. https://doi.org/10.1016/j.cub.2013.10.037 (2013).
20. Wardill, T. J. et al. Multiple spectral inputs improve motion discrimination in the *Drosophila* visual system. *Science* **336**, 925–931. https://doi.org/10.1126/science.1215317 (2012).
21. Helfrich-Forster, C. Light input pathways to the circadian clock of insects with an emphasis on the fruit fly *Drosophila melanogaster*. *J. Comp. Physiol. A. Neuroethol. Sens. Neural. Behav. Physiol.* **206**, 259–272. https://doi.org/10.1007/s00359-019-01379-5 (2020).
22. Kistenpfennig, C. et al. A new rhodopsin influences light-dependent daily activity patterns of fruit flies. *J. Biol. Rhythms.* **32**, 406–422. https://doi.org/10.1177/0748730417721826 (2017).
23. Helfrich-Forster, C. et al. The extraretinal eyelet of *Drosophila*: development, ultrastructure, and putative circadian function. *J. Neuroscience: Official J. Soc. Neurosci.* **22**, 9255–9266. https://doi.org/10.1523/JNEUROSCI.22-21-09255.2002 (2002).
24. Ni, J. D., Baik, L. S., Holmes, T. C. & Montell, C. A rhodopsin in the brain functions in circadian photoentrainment in *Drosophila*. *Nature* **545**, 340–344. https://doi.org/10.1038/nature22325 (2017).
25. Emery, P. et al. *Drosophila* CRY is a deep brain circadian photoreceptor. *Neuron* **26**, 493–504. https://doi.org/10.1016/s0896-6273(00)81181-2 (2000).
26. Emery, P., So, W. V., Kaneko, M., Hall, J. C. & Rosbash, M. CRY, a *Drosophila* clock and light-regulated cryptochrome, is a major contributor to circadian rhythm resetting and photosensitivity. *Cell* **95**, 669–679. https://doi.org/10.1016/s0092-8674(00)81637-2 (1998).
27. Stanewsky, R. et al. The cry[b] mutation identifies cryptochrome as a circadian photoreceptor in *Drosophila*. *Cell* **95**, 681–692. https://doi.org/10.1016/s0092-8674(00)81638-4 (1998).
28. Yoshii, T., Todo, T., Wulbeck, C., Stanewsky, R. & Helfrich-Forster, C. Cryptochrome is present in the compound eyes and a subset of *Drosophila*'s clock neurons. *J. Comp. Neurol.* **508**, 952–966. https://doi.org/10.1002/cne.21702 (2008).
29. Lazopulo, S., Lazopulo, A., Baker, J. D. & Syed, S. Daytime colour preference in *Drosophila* depends on the circadian clock and TRP channels. *Nature* **574**, 108–111. https://doi.org/10.1038/s41586-019-1571-y (2019).
30. Schümperli, R. A. Evidence for colour vision in *Drosophila melanogaster* through spontaneous phototactic choice behaviour. *J. Comp. Physiol.* **86**, 77–94 (1973).
31. Heisenberg, M. & Buchner, E. The role of retinula cell types in visual behavior of *Drosophila melanogaster*. *J. Comp. Physiol.* **117**, 127–162 (1977).
32. Hu, K. G. & Stark, W. S. Specific receptor input into spectral preference in *Drosophila*. *J. Comp. Physiol.* **121**, 241–252 (1977).
33. Jacob, K., Willmund, R., Folkers, E., Fischbach, K. & Spatz, H. C. T-maze phototaxis of *Drosophila melanogaster* and several mutants in the visual systems. *J. Comp. Physiol.* **116**, 209–225 (1977).
34. Fischbach, K. Simultaneous and successive colour contrast expressed in slow phototactic behaviour of walking *Drosophila melanogaster*. *J. Comp. Physiol.* **130**, 161–171 (1979).

35. Gao, S. et al. The neural substrate of spectral preference in *Drosophila*. *Neuron* **60**, 328–342. https://doi.org/10.1016/j.neuron.2008.08.010 (2008).
36. Yamaguchi, S., Desplan, C. & Heisenberg, M. Contribution of photoreceptor subtypes to spectral wavelength preference in *Drosophila*. *Proc. Natl. Acad. Sci. U.S.A.* **107**, 5634–5639. https://doi.org/10.1073/pnas.0809398107 (2010).
37. Hu, K. G. & Stark, W. S. The roles of *Drosophila* ocelli and compound eyes in phototaxis. *J. Comp. Physiol.* **135**, 85–95 (1980).
38. Harris, W. A., Stark, W. S. & Walker, J. A. Genetic dissection of the photoreceptor system in the compound eye of *Drosophila melanogaster*. *J. Physiol.* **256**, 415–439 (1976).
39. Vogt, K. et al. Shared mushroom body circuits underlie visual and olfactory memories in *Drosophila*. *eLife* **3**, e02395. https://doi.org/10.7554/eLife.02395 (2014).
40. Spatz, H. C., Emanns, A. & Reichert, H. Associative learning of *Drosophila melanogaster*. *Nature* **248**, 359–361 (1974).
41. Menne, D. & Spatz, H. C. Colour vision in *Drosophila melanogaster*. *J. Comp. Physiol.* **114**, 301–312 (1977).
42. Salomon, C. H. & Spatz, H. C. Colour vision in *Drosophila melanogaster*: wavelength discrimination. *J. Comp. Physiol. A: Neuroethology Sens. Neural Behav. Physiol.* **150**, 31–37 (1983).
43. Melnattur, K. V. et al. Multiple redundant medulla projection neurons mediate color vision in *Drosophila*. *J. Neurogenet.* **28**, 374–388. https://doi.org/10.3109/01677063.2014.891590 (2014).
44. Tang, S. & Guo, A. Choice behavior of *Drosophila* facing contradictory visual cues. *Science* **294**, 1543–1547 (2001).
45. Bicker, G. & Reichert, H. Visual learning in a photoreceptor degeneration mutant of *Drosophila melanogaster*. *J. Comp. Physiol.* **127**, 29–38 (1978).
46. Reichert, H. & Bicker, G. A visual learning study of brightness perception in two mutants of *Drosophila melanogaster*. *J. Comp. Physiol. A: Neuroethology Sens. Neural Behav. Physiol.* **133**, 283–290 (1979).
47. Benzer, S. Behavioral mutants of *Drosophila* isolated by countercurrent distribution. *Proc. Natl. Acad. Sci. U.S.A.* **58**, 1112–1119 (1967).
48. Kain, J. S., Stokes, C. & de Bivort, B. L. Phototactic personality in fruit flies and its suppression by serotonin and white. *Proc. Natl. Acad. Sci. U.S.A.* **109**, 19834–19839. https://doi.org/10.1073/pnas.1211988109 (2012).
49. Schnaitmann, C., Vogt, K., Triphan, T. & Tanimoto, H. Appetitive and aversive visual learning in freely moving *Drosophila*. *Front. Behav. Neurosci.* **4**. https://doi.org/10.3389/fnbeh.2010.00010 (2010).
50. Fukushi, T. Learning and discrimination of coloured papers in the walking blowfly, *Lucilia cuprina*. *J. Comp. Physiol. A.* **166**, 57–64 (1989).
51. An, L. et al. The yellow specialist: dronefly *Eristalis tenax* prefers different yellow colours for landing and proboscis extension. *J. Exp. Biol.* **221**. https://doi.org/10.1242/jeb.184788 (2018).
52. Zhu, E. Y., Guntur, A. R., He, R., Stern, U. & Yang, C. H. Egg-laying demand induces aversion of UV light in *Drosophila* females. *Curr. Biol.* **24**, 2797–2804. https://doi.org/10.1016/j.cub.2014.09.076 (2014).
53. Hori, M., Shibuya, K., Sato, M. & Saito, Y. Lethal effects of short-wavelength visible light on insects. *Sci. Rep.* **4**, 7383. https://doi.org/10.1038/srep07383 (2014).
54. Baik, L. S. et al. CRYPTOCHROME mediates behavioral executive choice in response to UV light. *Proc. Natl. Acad. Sci. U.S.A.* **114**, 776–781. https://doi.org/10.1073/pnas.1607989114 (2017).
55. Senthilan, P. R., Grebler, R., Reinhard, N., Rieger, D. & Helfrich-Forster, C. Role of rhodopsins as circadian photoreceptors in the *Drosophila melanogaster*. *Biology (Basel).* **8**. https://doi.org/10.3390/biology8010006 (2019).
56. Fukushi, T. Colour discrimination from various shades of grey in the trained blowfly, *Lucilia cuprina*. *J. Insect. Physiol.* **36**, 69–75 (1990).
57. Ramdya, P. et al. Mechanosensory interactions drive collective behaviour in *Drosophila*. *Nature* **519**, 233–236. https://doi.org/10.1038/nature14024 (2015).
58. Giurfa, M. Conditioning procedure and color discrimination in the honeybee *Apis mellifera*. *Die Naturwiss.* **91**, 228–231. https://doi.org/10.1007/s00114-004-0530-z (2004).
59. Koshitaka, H., Kinoshita, M., Vorobyev, M. & Arikawa, K. Tetrachromacy in a butterfly that has eight varieties of spectral receptors. *Proc. Biol. Sci.* **275**, 947–954. https://doi.org/10.1098/rspb.2007.1614 (2008).
60. Vogt, K. et al. Direct neural pathways convey distinct visual information to *Drosophila* mushroom bodies. *eLife* **5**. https://doi.org/10.7554/eLife.14009 (2016).
61. Ganguly, I., Heckman, E. L., Litwin-Kumar, A., Clowney, E. J. & Behnia, R. Diversity of visual inputs to Kenyon cells of the *Drosophila* mushroom body. *Nat. Commun.* **15**, 5698. https://doi.org/10.1038/s41467-024-49616-z (2024).
62. Menzel, R. & Backhaus, W. Color vision honey bees: phenomena and physiological mechanisms. *In Facets of Vision* 281–297 (Springer, 1989).
63. Frisch, K. v. Der farbensinn und Formensinn der Biene. (1914).
64. Arikawa, K. The eyes and vision of butterflies. *J. Physiol.* **595**, 5457–5464. https://doi.org/10.1113/JP273917 (2017).
65. Briscoe, A. D. Reconstructing the ancestral butterfly eye: focus on the opsins. *J. Exp. Biol.* **211**, 1805–1813. https://doi.org/10.1242/jeb.013045 (2008).
66. Kinoshita, M., Shimada, N. & Arikawa, K. Colour vision of the foraging swallowtail butterfly *Papilio xuthus*. *J. Exp. Biol.* **202**(Pt 2), 95–102 (1999).
67. Kelber, A. & Pfaff, M. True colour vision in the orchard butterfly, *Papilio aegeus*. *Die Naturwiss.* **86**, 221–224 (1999).
68. Kelber, A. & Henze, M. J. Colour vision: parallel pathways intersect in *Drosophila*. *Curr. Biology: CB.* **23**, R1043–1045. https://doi.org/10.1016/j.cub.2013.10.025 (2013).
69. Friedrich, M., Wood, E. J. & Wu, M. Developmental evolution of the insect retina: insights from standardized numbering of homologous photoreceptors. *J. Exp. Zool. B Mol. Dev. Evol.* **316**, 484–499. https://doi.org/10.1002/jez.b.21424 (2011).
70. Kind, E., Belušič, G. & Wernet, M. F. 1.08 - Retinal mosaics across fly species: variations on a theme. in *The Senses: A Comprehensive Reference (Second Edition)* (ed. FritzschM B.) 122–139 (Elsevier, 2020).
71. Giurfa, M., Vorobyev, M., Kevan, P. & Menzel, R. Detection of coloured stimuli by honeybees: minimum visual angles and receptor specific contrasts. *J. Comp. Physiol. A.* **178**, 699–709 (1996).
72. Giurfa, M., Vorobyev, M., Brandt, R., Posner, B. & Menzel, R. Discrimination of coloured stimuli by honeybees: alternative use of achromatic and chromatic signals. *J. Comp. Physiol. A.* **180**, 235–243 (1997).
73. Fukushi, T. Colour perception of single and mixed monochromatic lights in the blowfly *Lucilia cuprina*. *J. Comp. Physiol. A.* **175**, 15–22 (1994).
74. Shrestha, M. et al. Floral colours in a world without birds and bees: the plants of Macquarie Island. *Plant. Biol. (Stuttg).* **18**, 842–850. https://doi.org/10.1111/plb.12456 (2016).
75. Arnold, S. E., Savolainen, V. & Chittka, L. Flower colours along an alpine altitude gradient, seen through the eyes of fly and bee pollinators. *Arthropod-Plant Interact.* **3**, 27–43 (2009).
76. Ohashi, K., Makino, T. T. & Arikawa, K. Floral colour change in the eyes of pollinators: testing possible constraints and correlated evolution. *Funct. Ecol.* **29**, 1144–1155 (2015).
77. Vorobyev, M. & Osorio, D. Receptor noise as a determinant of colour thresholds. *Proc. Biol. Sci.* **265**, 351–358. https://doi.org/10.1098/rspb.1998.0302 (1998).
78. Heath, S. L. et al. Circuit mechanisms underlying chromatic encoding in *Drosophila* photoreceptors. *Curr. Biol.* **30**, 264–275 e268, (2020). https://doi.org/10.1016/j.cub.2019.11.075

79. Garbers, C. & Wachtler, T. Wavelength discrimination in *Drosophila* suggests a role of rhodopsin 1 in color vision. *PloS One*. **11**, e0155728. https://doi.org/10.1371/journal.pone.0155728 (2016).
80. Schnaitmann, C. et al. Color processing in the early visual system of *Drosophila*. *Cell* **172**, 318–330 e318, https://doi.org/10.1016/j.cell.2017.12.018 (2018).
81. Yonekura, T., Yamauchi, J., Morimoto, T. & Seki, Y. Spectral response properties of higher visual neurons in *Drosophila melanogaster*. *J. Comp. Physiol. A. Neuroethol. Sens. Neural. Behav. Physiol.* **206**, 217–232. https://doi.org/10.1007/s00359-019-01391-9 (2020).
82. Christenson, M. P. et al. Hue selectivity from recurrent circuitry in *Drosophila*. *Nat. Neurosci.* **27**, 1137–1147. https://doi.org/10.1038/s41593-024-01640-4 (2024).
83. Li, Y. et al. Neural mechanism of spatio-chromatic opponency in the *Drosophila* amacrine neurons. *Curr. Biol.* https://doi.org/10.1016/j.cub.2021.04.068 (2021).
84. Pagni, M. et al. Interaction of chromatic and achromatic circuits in *Drosophila* color opponent processing. *Curr. Biol.* https://doi.org/10.1016/j.cub.2021.01.105 (2021).
85. Matsliah, A. et al. Neuronal parts list and wiring diagram for a visual system. *Nature* **634**, 166–180. https://doi.org/10.1038/s41586-024-07981-1 (2024).

Acknowledgements

Author contributions

Y.S. conceived the study and wrote the manuscript. Y.S. and Y.T. designed the experiments. Y.S., Y.T., T.Y., A.T., and M.M. performed the experiments and collected data. Y.S. interpreted and analyzed data. T.M. and J.Y. assisted with data interpretation and edited the manuscript.

Declarations

Competing interests

The authors declare no competing interests.

Additional information

Supplementary Information The online version contains supplementary material available at https://doi.org/10.1038/s41598-025-19946-z.

Correspondence and requests for materials should be addressed to Y.S.

Reprints and permissions information is available at www.nature.com/reprints.

Publisher's note Springer Nature remains neutral with regard to jurisdictional claims in published maps and institutional affiliations.